

## Breakdown of Kramers theory description of photochemical isomerization and the possible involvement of frequency dependent friction

Stephan P. Velsko, David H. Waldeck, and Graham R. Fleming

Citation: *The Journal of Chemical Physics* **78**, 249 (1983); doi: 10.1063/1.444549

View online: <http://dx.doi.org/10.1063/1.444549>

View Table of Contents: <http://scitation.aip.org/content/aip/journal/jcp/78/1?ver=pdfcov>

Published by the [AIP Publishing](#)

---

### Articles you may be interested in

[Velocity dependence of friction and Kramers relaxation rates](#)

*J. Chem. Phys.* **126**, 244501 (2007); 10.1063/1.2740257

[Is slow thermal isomerization in viscous solvents understandable with the idea of frequency dependent friction?](#)

*J. Chem. Phys.* **102**, 9565 (1995); 10.1063/1.468772

[The effect of frequency dependent friction on isomerization dynamics in solution](#)

*J. Chem. Phys.* **78**, 2735 (1983); 10.1063/1.444983

[Friction and velocity in Kramers' theory of chemical kinetics](#)

*J. Chem. Phys.* **72**, 1392 (1980); 10.1063/1.439204

[Theory of photochemical isomerization in polyenes](#)

*J. Chem. Phys.* **64**, 1612 (1976); 10.1063/1.432333

---



## Re-register for Table of Content Alerts

Create a profile.



Sign up today!



# Breakdown of Kramers theory description of photochemical isomerization and the possible involvement of frequency dependent friction

Stephan P. Velsko,<sup>a)</sup> David H. Waldeck, and Graham R. Fleming<sup>b)</sup>

*James Franck Institute and Department of Chemistry, The University of Chicago, Chicago, Illinois 60637*

(Received 10 December 1981; accepted 29 September 1982)

We present new data on the ground state isomerization rate of DODCI and compare our results to previously obtained excited state data. We find that the one-dimensional Kramers expression does not fit the data over the whole viscosity range when the friction is measured by either the overall rotation time or the solvent viscosity. The deviation is qualitatively similar to that previously observed in diphenyl butadiene when the viscosity was used as the friction measure. Deviations from the simple hydrodynamic theory appear to depend on the reduced frequency for isomerization. We show how our results are consistent with the one-dimensional Kramers theory when a frequency dependent friction is used to describe the influence of the solvent.

## I. INTRODUCTION

Radiationless processes involving large amplitude motion, such as photochemical isomerization processes in molecules where bulky groups must twist with respect to a molecular axis, should have rates which depend on the frictional forces exerted by the solvent. Before the detailed way in which solvent friction effects isomerization can be understood, several questions must be answered: To what extent is a one-dimensional barrier crossing picture applicable to the photoisomerizations of large molecules in solution? What assumptions about the relative timescales for isomerization per se, for the velocity relaxation of the isomerization coordinate, and for the correlations among forces exerted by the solvent are valid? How accurate are simple hydrodynamic models for the microscopic motions involved in isomerization? In a recent study of diphenyl butadiene (DPB) in alkane solvents<sup>1</sup> we found that the Kramers expression<sup>2</sup> with hydrodynamic friction did not fit the viscosity dependence of the twisting rate well. If the low viscosity points are fit to a Kramers expression the experimental high viscosity points lie at higher rates than the theory predicts. Conversely, fitting to the high viscosity points causes the theoretical curve to undershoot the experimental data at low viscosity. In other words, the Kramers expression does not have the correct qualitative shape to reproduce the apparent viscosity dependence. Similar behavior is observed by Hochstrasser and co-workers for stilbene.<sup>3</sup> In our study of DPB we suggested that it may be necessary to consider the frequency dependence of the medium viscosity.<sup>1,4</sup> It is also possible that the one-dimensional picture assumed in the Kramers expression is inappropriate for molecules such as the diphenyl polyenes and that a multidimensional theory is necessary.<sup>3</sup> Finally, a possible complication in measurements involving electronically excited states is that solvent independent competing relaxation processes, if not cor-

rectly accounted for, may distort the apparent viscosity dependence.<sup>5</sup>

Our earlier study of isomerization rates in the excited singlet state of the cyanine dye DODCI(3,3'-diethyl-oxadiazocyanine iodide),<sup>6</sup> together with the ground state isomerization data presented in this paper, provide us with an opportunity to explore these ideas further. Comparison of the ground and excited state isomerization rates as a function of viscosity shows them to be qualitatively alike and implies that our previous analysis of the excited state kinetics is valid. In addition to the possibility of comparing the isomerization process in the excited and ground states, we are also able to consider the frictional forces in detail since we possess data on the viscosity and temperature dependence of the rotational diffusion of DODCI in the ground state.<sup>7</sup> We analyze our results in the context of the one-dimensional barrier crossing picture. By comparing data for several molecules we show that the effective friction for the isomerization process is strongly dependent on the presence of the potential barrier. A frequency dependent friction may explain the pattern of viscosity dependence observed for these molecules.

First, we briefly outline the experimental methods used. In Sec. III we present the results for ground state isomerization and discuss some aspects of the observed behavior. In Sec. IV, we discuss several models for isomerization and their applicability to our results, concentrating on possible reasons for the failure of the one-dimensional hydrodynamic Kramers expression to fit our data. Particular attention is paid to the effective solvent friction. Section V contains some concluding remarks.

## II. EXPERIMENTAL

The DODCI was obtained from Eastman-Kodak and all solvents were analytic grade from Aldrich. Sample thermostating was accomplished with a brass cooling block and a Neslab RTE-4 circulating bath. The sample

<sup>a)</sup> Present address: Department of Chemistry, University of Pennsylvania, Philadelphia, Pennsylvania 19174.

<sup>b)</sup> Alfred P. Sloan Foundation Fellow.

TABLE I. Isomerization lifetimes.

Solvent	$T(K)^a$	$\eta(\text{cp})^b$	$\tau(\text{ms})$
EtOH	294.6	1.16	3.01
PrOH	295.6	2.09	4.21
ButOH	294.5	2.85	4.60
PeOH	294.5	4.00	5.43
HexOH	295.6	4.93	6.26
OctOH	295.5	8.17	5.51
DeCOH	294.6	13.47	6.43

<sup>a</sup> $T$  values are accurate to  $\pm 0.5$  K.

<sup>b</sup> $\eta$  values obtained by least squares fit to an Arrhenius plot of values from Ref. 8.

temperature was monitored with a digital thermometer (OMEGA 199) using a copper-constantan thermocouple.

A conventional flash photolysis technique was used to obtain the ground state isomerization rate. DODCI when excited to its first singlet state rapidly (few nanoseconds) relaxes to the ground state with approximately 10% production of an isomeric form. This isomer can be distinguished from the normal form by its absorption spectrum and relaxes to the normal form via a thermally assisted barrier crossing on a microsecond to millisecond timescale. The excitation source was an electrophotonics flashlamp pumped dye laser with a pulse width of 20  $\mu\text{s}$ . The laser dyes used in these studies were coumarin 480 and rhodamine 6G, and the isomerization rate was observed to be independent of excitation wavelength. The analyzing light source operated at low intensity through a Schott RG630 cutoff filter and at 90° to the excitation source. The modulation of the analyzing light was detected through a 630 nm interference filter by a 1P28 phototube whose output was checked for linearity in analyzing light intensity. The output from the phototube was stored in a Biomation model 805 waveform recorder, which was calibrated using a square wave generator of known frequency, and subsequently loaded into a Vax 11/780 computer.

In addition to the wavelength independence stated earlier, the observed rates were also found to be in-

dependent of our laser intensity and the percent modulation of the analyzing light which was never greater than 80%. Furthermore, no difference for the rate was observed in aerated vs deaerated solvents.

### III. RESULTS

#### A. Observed rates

Measured isomerization decay times for DODCI in normal alcohols are listed in Table I. The viscosities listed are obtained from an Arrhenius fit (see Table II) to viscosity data found in Ref. 8. The temperature listed in Table I is estimated to have an error of 0.5 degrees, and at  $T = 294$  K such an error introduces an uncertainty in the lifetime of approximately 10% because of the large activation energy for this process.

A representative decay profile is shown in Fig. 1. The observed signal was converted to the proper exponential form using Beers law<sup>9</sup>

$$-\log_{10} \frac{I_{tr}(t)}{I_0} = \epsilon C(t)l,$$

where  $C(t)$  is the time dependent concentration of photo-isomer,  $l$  is the path length,  $\epsilon$  is the extinction coefficient,  $I_0$  is the incident intensity, and  $I_{tr}(t)$  is the transmitted intensity at time  $t$ . A value of  $I_0$  was obtained by measuring the transmitted intensity at long time; this assumes that the absorbance of the normal form at 630 nm is negligible. After the decay profiles were transformed into exponential form, they were fit to a single exponential. All fits were over a range of two to four  $1/e$  times. Although fewer than 5% of our fits gave reasonable values for the statistical "runs" test,<sup>10</sup> decays which failed the runs test yielded lifetimes which were very close to lifetimes obtained from decays which passed, when the decays were obtained under the same experimental conditions. In other words, the systematic errors which were present did not greatly influence the fitted lifetime. The error in the fitted lifetimes is dominated by the error introduced by the uncertainty in the temperature, 10%.

The decay times listed in Table I seem to agree well with those of Jaraudias.<sup>11</sup> Although our values are consistently longer than Jaraudias', the discrepancy is

TABLE II. Arrhenius parameters for the solvent viscosity, isomerization, and overall rotation.<sup>a</sup>

Solvent	$E_{\eta}(\frac{\text{kcal}}{\text{mol}})$	$\eta_0 (10^{-3} \text{ cp})$	$E_{iso}^{\ddagger}(\frac{\text{kcal}}{\text{mol}})$	$A_{iso}^{\ddagger} (10^{12} \text{ s}^{-1})$	$E_{iso}^{\circ}(\frac{\text{kcal}}{\text{mol}})$	$A_{iso}^{\circ} (10^{12} \text{ s}^{-1})$	$E_{or}(\frac{\text{kcal}}{\text{mol}})$	$A_{or} (10^{12} \text{ s}^{-1})$
Ethanol	3.58	2.6	14.7	23	$5.45 \pm 0.55$	6.3	$4.2 \pm 0.2$	0.026
Propanol	4.24	1.5	14.7	17	...	...		
Butanol	4.59	1.1	15.4	48	$5.41 \pm 0.39$	4.1	$4.9 \pm 0.3$	0.040
Pentanol	5.49	0.34	14.4	9.3	$5.31 \pm 0.71$	3.1		
Hexanol	5.32	0.60	14.8	15	$5.64 \pm 0.67$	4.6		
Octanol	6.42	0.14	14.6	12	...	...		
Decanol	6.70	0.14	15.7	67	$6.09 \pm 0.83$	8.4	$7.4 \pm 0.7$	0.062

<sup>a</sup>g—ground state; e—excited state; iso—isomerization; or—overall rotation;  $\eta$ —viscosity.

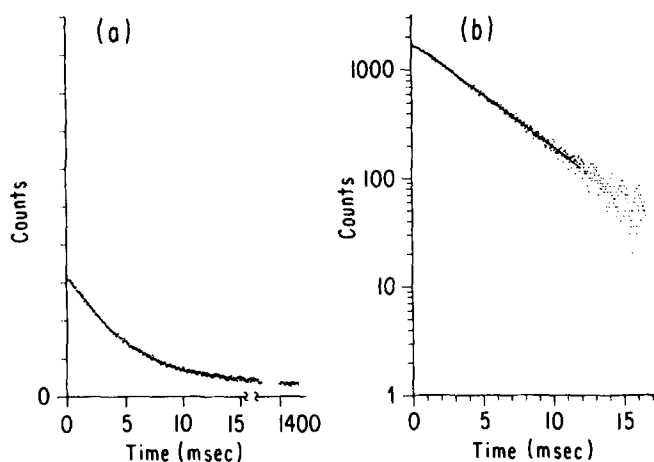


FIG. 1. A representative decay curve for DODCI in butanol at 23°C is shown. Figure 1(a) is the observed flash photolysis signal where the high number of counts at very long times (note break in  $x$  axis) is caused by blocking the probe light and is  $I_0$ . In Fig. 1(b) the same curve is shown after conversion to exponential form. Also, the fitted curve is drawn through the points.

on the order of the experimental uncertainty. In contrast, our value of  $\tau_{iso}$  in ethanol is larger than the values obtained by Dempster<sup>9</sup> and Rulliere<sup>12</sup> by approximately a factor of 2. We have no explanation for this discrepancy.

### B. Arrhenius plots

Figure 2 displays Arrhenius plots of the isomerization rate in ethanol and decanol. It is evident that over our temperature range the plots are linear; implying that there is no other process depleting the photoisomer population, in contrast to the excited state case where the plots showed a definite curvature at low temperature.<sup>6</sup> Fits of the data to the Arrhenius form yield activation energies and frequency factors for the isomerization process. The fitted parameters are listed in Table II with the Arrhenius parameters for the ex-

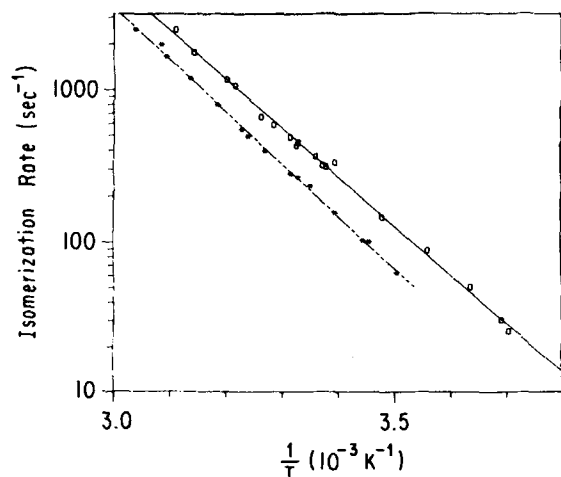


FIG. 2. Arrhenius plots of the data are shown for ethanol (○) and decanol (\*).

cited state isomerization rate,<sup>6</sup> the overall rotational diffusion of DODCI,<sup>7</sup> and the solvent viscosity<sup>8</sup> which is fit to the form  $1/\eta = (1/\eta_0)e^{-\epsilon\eta/RT}$ . We note that the value obtained for the activation energy of the ground state isomerization in ethanol is in good agreement with the previous determination of this parameter by Rulliere.<sup>12</sup>

The activation energies for the isomerization process in the ground state are three times larger than those observed in the excited state. This large difference probably occurs because of the change in the amount of pi-bond conjugation between the ground and excited states. Although the absolute values of the activation energies in the ground and excited state differ greatly, within our experimental error they seem equally insensitive to the solvent as one progresses through the series of normal alcohols from ethanol to decanol. This behavior is in contrast to that seen in the overall rotational diffusion where the activation energies, although only three in number, seem to scale with the solvents viscosity activation. This difference in behavior will be discussed in more detail later.

### C. Isoviscosity plots

As previously mentioned,<sup>1,6</sup> we assume that the isomerization rate takes the form

$$k_{iso} = F(\eta) \exp(-E_0/RT), \quad (1)$$

where  $F(\eta)$  is a universal function of viscosity and  $E_0$  is an intrinsic molecular barrier height. By plotting  $\ln(k_{iso})$  vs  $1/T$  at constant viscosity, one obtains a value for  $E_0$ . Two of these isoviscosity plots are shown in Fig. 3, and the Arrhenius parameters obtained from plots of this type at various viscosities are presented in Table III. The average  $E_0$  obtained in this manner is 13.7 kcal/mol. The data listed in Table III might imply that the internal barrier which one obtains at low viscosities differs from the one obtained at high viscosities because of differing solvents. We have not attributed any significance to this very weak bimodal character since the value of  $E_0$  can change by nearly a kcal, de-

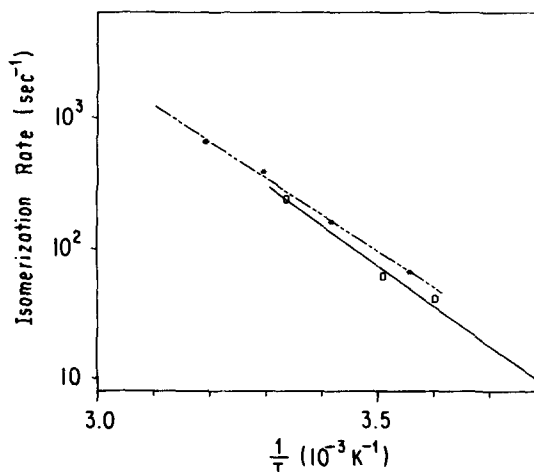


FIG. 3. Isoviscosity plots are displayed for  $\eta = 3$  cp (\*) and  $\eta = 7$  cp (○).

TABLE III. Arrhenius parameters from iso-viscosity plots.

Viscosity	$E_0^{\ddagger}$ (kcal/mol)	$A^{\ddagger}$ ( $s^{-1}$ )
1 cp	13.5	$2.9 \times 10^{12}$
2 cp	12.9	$0.90 \times 10^{12}$
3 cp	13.1	$1.0 \times 10^{12}$
5 cp	14.0	$4.0 \times 10^{12}$
7 cp	14.4	$8.4 \times 10^{12}$
9 cp	14.1	$4.7 \times 10^{12}$

pending on the number of points plotted. This value of 13.7 kcal/mol is five times greater than the value of 2.7 kcal/mol determined for the internal barrier to isomerization in the excited state<sup>6</sup> and is the factor most responsible for the  $10^5$  difference in ground and excited state rates. In subsequent calculations we use the average value of 13.7 kcal/mol for the height of the internal barrier to isomerization in the ground state.

#### D. Reduced isomerization rates

The reduced isomerization rate, defined as

$$k_{iso}^* = k_{iso} e^{E_0/R T} \quad (2)$$

differs by less than an order of magnitude in the ground ( $k_{iso}^{*g}$ ) and excited ( $k_{iso}^{*e}$ ) states. Also, the dependence of  $k_{iso}^{*g}$  and  $k_{iso}^{*e}$  on the viscosity are qualitatively the same. This similarity is only qualitative, however, and we will show that they differ in quantitative detail. With the above definition of  $k_{iso}^*$  we may try to isolate the effect of the barrier height upon the isomerization rate from the effect of the solvent and other characteristics

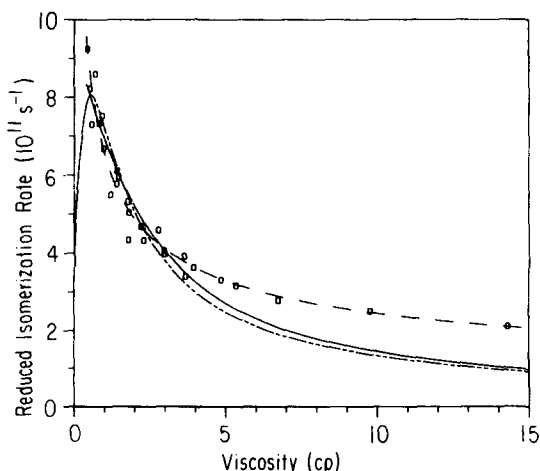


FIG. 4. A plot of reduced rate vs viscosity for the excited state data. The solid line is a fit of the Kramers function to all of the points. The dotted line is a fit of the Skinner and Wolynes function [Eq. (18)] to all the points. The dashed line is a fit to an expression of the form  $k^* \propto (\eta^a)^{-1}$ . The value of  $a$  is 0.43. An excellent fit to this form is also obtained to the ground state data with  $a = 0.26$ .

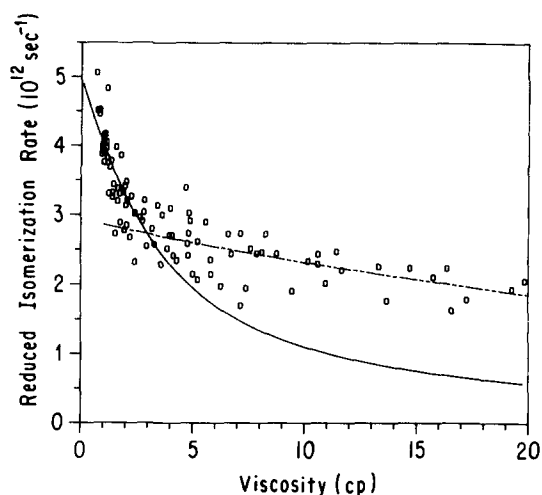


FIG. 5. A plot of the reduced rate vs viscosity for the ground state data. The solid line is the Kramers function obtained by fitting to data points  $< 4$  cp. The dotted line is obtained by fitting the same function to points  $> 10$  cp.

of the potential. We have done this in Figs. 4 and 5 by plotting  $k_{iso}^*$  vs  $\eta$  for both the excited and ground states, respectively. The excited state plot has fewer data points because we were limited to the use of only high temperature values because of the presence of the low temperature nonradiative decay channel.<sup>6</sup>

The results in Figs. 4 and 5 show that when the temperature dependence of the isomerization rate due to the internal barrier ( $E_0$ ) is removed, the magnitudes of the resulting "reduced rates"  $k_{iso}^*$  are well correlated with solvent viscosity. The reduced rates at the same viscosity are approximately equal, independent of the means by which that viscosity value was produced, i.e., by changing the temperature or the solvent.

We should point out, however, that although this "universal" viscosity dependence holds to a good approximation in the series of linear alcohols, it may not extend to solvents outside the series. The origin of such "specific solvent effects" is not yet well understood but two possible causes are:

(a) Static modifications of the potential surface.  $E_0$  is rigorously related to a solvent dependent "potential of mean force." An example of a strong solvent effect of this sort is seen in the case of diphenyl butadiene, which has an  $E_0$  of 4.7 kcal/mol in alkanes but an  $E_0 \sim 0.5$  kcal/mol in alcohols.<sup>13</sup>

(b) "Boundary condition" effects in which solvent molecular size or structure affects the frictional coupling strength to the isomerization coordinate.

A natural question is whether such effects might be operating *within* the series of linear alcohols. We can exclude a direct effect on the barrier height from our iso-viscosity plots for the ground and excited state<sup>6</sup> data. We will address the question of boundary conditions in a later section. In any case, if such effects are in force, Figs. 4 and 5 show they must be strongly correlated with viscosity in the series of linear alcohols.

#### IV. DISCUSSION

In this section, we discuss several features of one-dimensional, barrier crossing models for isomerization and compare them with our data. We include a comparison of our data and other data for viscosity controlled large amplitude molecular motion.

##### A. Brownian motion theories of isomerization

Recently there has been a great revival of theoretical interest in the one-dimensional barrier crossing problem, and its applications to photochemical isomerization.<sup>17-19</sup> The Kramers expression (3):

$$k_{\text{iso}} = \frac{\omega_0}{4\pi\omega'\tau_v} [(1 + (2\omega'\tau_v)^2)^{1/2} - 1] e^{-E_0/RT} \quad (3)$$

is an approximate expression for the flux of population across a barrier assuming that the time dependent distribution of isomerization coordinates and velocities obey a Fokker-Planck equation. In expression (3)  $\omega_0$  is the frequency of the potential well of the initial minimum,  $E_0$  is the barrier height, and  $\omega'$  is the frequency of the barrier maximum.<sup>2</sup> A fundamental supposition of this description is that the forces acting on the isomerization coordinate relax very quickly compared to the velocity relaxation time ( $\tau_v$ ) of the coordinate. This "delta correlated" force assumption underlies all Brownian motion theories of molecular motion.<sup>20</sup> In the Brownian motion theory,  $\tau_v$  is related to the friction coefficient  $\zeta$  by

$$\tau_v = \mu/\zeta \quad (4)$$

with  $\mu$  being the effective mass of the coordinate. Given the Fokker-Planck (Brownian motion) description of the motion, there are two natural dynamical limits to consider. The first is where the momentum relaxation time  $\tau_v$  is very long compared to "free motion" timescales, i.e., the frictional forces are a small perturbation on the free motion. In this case, the rate of isomerization ought to be proportional to the friction.<sup>2,17-19</sup> In this respect, expression (3) is incorrect, since it becomes independent of  $\zeta$  in this limit. This feature of the Kramers expression has proven unimportant for our results since we find that the isomerization rate always decreases with increasing viscosity. The other case to consider is when the friction is very large, and  $\tau_v$  is short compared with the characteristic time scales of free motion on the potential surface. This is called the "Smolukchowski limit" and

$$k_{\text{iso}} \sim (1/\zeta) e^{-E_0/RT}. \quad (5)$$

These two limits of the Kramers problem are analogous to the "inertial" and "diffusive" limits of the free rotation problem.

It is common to assume a hydrodynamic model for  $\zeta$  in which

$$\zeta \propto \eta, \quad (6)$$

so that hydrodynamic Kramers expression can be written

$$k_{\text{iso}}^* = \frac{A}{B/\eta} [(1 + (B/\eta)^2)^{1/2} - 1], \quad (7)$$

where  $A = \omega_0/2\pi$  and  $B/\eta = 2\omega'\tau_v$ . This hydrodynamic model, which provides the rationale for plotting  $k_{\text{iso}}^*$  vs  $\eta$ , is quite distinct from the stochastic assumptions which result in the more general expression (3).

We have performed a nonlinear least squares fit of the isomerization data to Eq. (7). We found that the hydrodynamic Kramers expression does not have the correct shape to fit our data, and that both the excited state and ground state data deviate from predicted Kramers behavior in the same way. This deviation is shown in Fig. 5 where we have fit the ground state data to the hydrodynamic Kramers expression. The solid line is a fit of the data for  $\eta < 4$  cp and is seen to undershoot the observed rate at high viscosity, while the dotted line is a fit of the data for  $\eta > 10$  cp and is seen to undershoot the observed rate at low viscosity. It is clear from Fig. 5 that the Kramers expression (7) does not fit the data well over the full range. The solid curve in Fig. 4 is the best fit of the Kramers expression to the excited state data over the full viscosity range and the resultant Kramers parameters are  $\omega_0 = 6.0 (\pm 0.5) \times 10^{12} \text{ s}^{-1}$  and  $\omega'\tau_v = 1.6 (\pm 0.2)$ . Although the hydrodynamic Kramers equation does not fit the data well, the parameter  $A$  was found to change by less than a factor of 2 over any fitting range. We have also performed a fit of this type for the ground state data, and although not shown it has a behavior qualitatively similar to the excited state data. The Kramers parameters from the best fit to the ground state data are  $\omega_0 = 2.5 (\pm 0.1) \times 10^{13} \text{ s}^{-1}$  and  $\omega'\tau_v = 7.6 (\pm 1.6) \text{ cp}$ . A comparison of these parameters for the two cases and the assumption that  $\tau_v$  is the same in both states implies that the potential well and barrier in the ground state are a factor of 4 to 5 sharper than those in the excited state.

The Kramers parameters obtained above imply that the isomerization process is not in the Smoluchowski limit since  $\omega'\tau_v$  is not much less than unity. The Arrhenius plots of the rate are a further indication that we are not in the Smoluchowski limit, because the observed activation energy is seen to be less than the sum of the internal barrier and the viscosity activation energy (Table II). In the context of Kramers theory, we conclude that DODCI isomerization in *n*-alcohols is in the intermediate friction region since the rate decreases with viscosity but not as  $1/\eta$ . This is the case for both the ground and excited states, although the ground state isomerization rate is seen to have a weaker dependence on the viscosity than the excited state isomerization rate.

At this point, we mention that excellent fits of the reduced rate for DODCI to the functional form  $D/\eta^a$  are obtained. The dashed line in Fig. 5 shows the fit for the excited state data with  $a = 0.43$ . A similarly good fit is obtained for the ground state data (not shown) with  $a = 0.26$ . This was also true for our DPB data, when  $a = 0.59$ .<sup>1</sup> This power dependence on viscosity with  $a < 1$  has been observed by other workers in differ-

ent types of molecules under various conditions of temperature, pressure, and solvent and has been given several distinct interpretations.<sup>14-16</sup> Since this  $a$  parameter is sometimes related to the volume of the isomerizing moiety and the volume of solvent it must displace, we would expect the ground state  $a$  value to be larger than the excited state value of  $a$  for DODCI. This is because in excited state DODCI, the "transition state" occurs at 1/2 the angular displacement it occurs at for ground state DODCI. Therefore, the total twisting motion necessary for isomerization in excited state DODCI is roughly one-half the motion necessary for ground state isomerization. We present no explanation for this failure in terms of these models, but will discuss it later in the context of frequency dependent friction.

### B. Approach of Skinner and Wolynes (SW)

An approximate expression for the isomerization rate which interpolates between the correct low, but non-zero, friction limit and the diffusive limit has been derived by Skinner and Wolynes.<sup>17</sup> The expression is

$$k = A' gT \left[ 1 + \frac{gT}{2} + \frac{(gT)^2}{2\pi} \right]^{-1} e^{-E_0/RT}, \quad (8)$$

where frequencies of the potential well and barrier are assumed equal and to compare with the Kramers formula  $gT = (2\pi/(\omega' \tau_v))$  and  $A' = \omega'/2\pi$ . This functional form is seen to deviate from the data in a manner similar to the hydrodynamic Kramers expression (7). An example of the best fit of Eq. (8) to the excited state data is seen in Fig. 4; the parameters are  $\omega' = 6.5 \times 10^{12} \text{ s}^{-1}$  and  $\omega' \tau_v = 1.4$  at 1 cp. This function was also fit to the ground state data where the fit was worse than that shown for the excited state; the parameters are  $\omega' = 3.1 \times 10^{13} \text{ s}^{-1}$  and  $\omega' \tau_v = 3.7$  at 1 cp. These parameters suggest, as the Kramers parameters do, that the potential surface for the ground state isomerization process has a sharper barrier than the potential surface for the excited state isomerization process.

It should be noted that for DPB in alkanes there was no detectable difference between the fitted Kramers curve and the SW curve.<sup>1</sup> However, as Fig. 4 shows, in the case of DODCI excited state isomerization, the two curves are noticeably different. The ground state isomerization rate shows an even larger difference between the Kramers and the SW curve. The expression of Wolynes and Skinner is expected to differ from Kramers in the low and intermediate friction regions, and the differences between the two curves in the various cases—DODCI ground state, DODCI excited state, DPB excited state—is evidence that these isomerization processes are in the intermediate friction region. From the relative discrepancies in the fitted curves for the three cases and the values of  $\omega' \tau_v$  obtained from the fits, we would conclude that the DODCI ground state process in alcohols is furthest away from the high viscosity region and the DPB excited state process in alkanes is closest to the high viscosity region.

### C. Analysis of the friction

It is clear from Figs. 4 and 5 that Eq. (7) does not account for the curvature in our data. We have seen the same qualitative deviation from the Kramers expression for the isomerization rate of DPB in the alkanes. A major point at which Eq. (7) may break down is the hydrodynamic expression for  $\zeta$ , Eq. (6). To test the hydrodynamic expression for the friction, one clearly needs some other, independent measure of the "friction"  $\zeta$  felt by the isomerization. It seems reasonable to suggest that whatever the nature of the forces which inhibit them, the rotational and isomerization motions ought to feel frictions which are proportional to each other, *if the Brownian motion assumption holds*, i.e., if the zero frequency friction is the appropriate quantity to use in expression (3). Gillbro and Sundström<sup>21</sup> have recently noted that in different solvents of the same viscosity one observes differences in rotational diffusion rates of xanthene dyes which parallel differences seen in the isomerization rates of certain cyanine dyes. While they were not able to quantify this relationship, we can make such a comparison since we possess both isomerization and rotational diffusion data for DODCI.

In the rotational diffusion limit, the rotational diffusion time is related to the medium friction coefficient by the Hubbard relation<sup>22</sup>:

$$\tau_{\text{rot}} = \frac{I \zeta_{\text{or}}}{6kT} \quad (9)$$

The assumption of rotational diffusion for DODCI is evidently justified by the excellent fit to single exponential kinetics implied by the rotational diffusion model, and the rather long reorientation times which are observed ( $\geq 100$  ps). We do not, however, assume a model for  $\zeta$ . Instead, we postulate that the friction for isomerization is simply proportional to that for rotational motion:

$$\zeta_{\text{iso}} = f \zeta_{\text{or}}, \quad (10)$$

where  $f$  is the proportionality constant. Our data on the rotational diffusion times were obtained as a function of temperature, and so in order to make use of Eq. (9) in Eq. (10) we need to remove the intrinsic temperature dependence from  $\tau_{\text{rot}}$ . We define a reduced reorientation rate  $\tau_{\text{rot}}^*$  as

$$\tau_{\text{rot}}^* = \tau_{\text{rot}} P; \quad P = (I/\hbar^2) kT, \quad (11)$$

where  $P$  is a dimensionless quantity proportional to  $kT$ . Combining Eq. (11) with Eqs. (9) and (10) leads to

$$\zeta_{\text{iso}} = \frac{6f\hbar^2 \tau_{\text{rot}}^*}{I^2} \quad (12)$$

In the Kramers expression we define a similarly reduced isomerization rate  $k_{\text{iso}}^*$  as in expression (2).

Given the Kramers expression (3) we have

$$k_{\text{iso}}^* = \frac{\omega_0}{4\pi\omega' \tau_v} \left[ (1 + (2\omega' \tau_v)^2)^{1/2} - 1 \right]. \quad (13)$$

If in expression (13)  $\tau_v = \mu/\zeta_{\text{iso}}$  and  $2\omega' \tau_v = C/\tau_{\text{rot}}^*$  then

our final expression based on the postulate of Eq. (9) is

$$k_{\text{iso}}^* = \frac{A\tau_{\text{rot}}^*}{C} \left[ 1 + (C/\tau_{\text{rot}}^*)^2 \right]^{1/2} - 1. \quad (14)$$

By using expression (14) we can avoid the assumption of a hydrodynamic model for  $\tau_v$ , when testing the Kramers expression (3).

Figure 6 shows the reduced rotational diffusion data of Ref. 7 plotted against viscosity. The solid line shows the least squares fit to the expression

$$k_{\text{rot}}^* = D/\eta^a, \quad (15)$$

where  $a$  and  $D$  are parameters and  $k_{\text{rot}}^*$  is  $\tau_{\text{rot}}^{*-1}$ . An excellent fit is obtained and for the rotational diffusion data  $a$  is very close to unity ( $a=0.99$ ). A value of  $a=0.99$  corresponds to the simple inverse viscosity dependence of the Stokes-Einstein relation, a result in accord with our previous conclusion that simple hydrodynamics provides a good description of the rotational motion of DODCI.<sup>7</sup>

We have fit the isomerization data to Eq. (14) and observed that the very small deviation from Stokes law in the rotational diffusion rate is not enough to explain the breakdown of (3); the fit of  $k_{\text{iso}}^*$  vs  $\tau_{\text{or}}^*$  is qualitatively the same as the fit of  $k_{\text{iso}}^*$  against viscosity. This certainly implies that if the one-dimensional model is correct then, in a sense, rotations feel a different friction than isomerizations.

#### D. Boundary conditions<sup>23-26</sup>

The possibility of a "saturation" in the retarding influence of solvent viscosity on the rate of rotational reorientation has been discussed from a number of viewpoints.<sup>23,24</sup> As the solvent molecular size increases with respect to the solute, it has been suggested that a transition from a stick boundary condition to a slip boundary condition may occur.<sup>23</sup> An earlier study reported such an effect for the rotational diffusion of rhodamine 6G in very viscous solutions<sup>23</sup> but more

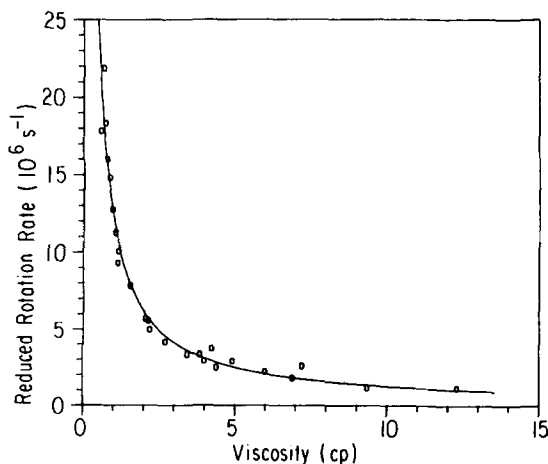


FIG. 6. Plot of the reduced rotational diffusion rate vs viscosity. The dotted line is the fit of Eq. 1 to the data with  $a = 0.99$ .

TABLE IV. Summary of barrier crossing data.

System	Barrier height (kcal)	Effective frequency at 1 cp ( $s^{-1}$ )	$\omega' \tau_v$ at 1 cp	$a^b$
DODCI				
GS	13.7	$4 \times 10^{12}$	7.5	0.26
ES	2.7	$8 \times 10^{11}$	0.8	0.43
[Rotation]	0	$10^7$	...	0.99
DPB				
ES alkanes	4.7	$1.5 \times 10^{12}$	0.71	0.69
ES alcohols	~0.5	$1.5 \times 10^{10}$	... <sup>a</sup>	0.92
Fav 2R				
ES (alcohols) (Ref. 16)	~0.2	$9 \times 10^{10}$	... <sup>a</sup>	0.98

<sup>a</sup>In the Smoluchowski limit only the product  $\omega_0 \omega' \tau_v$  is significant (Ref. 13).

<sup>b</sup>Obtained from  $k \propto (1/\eta^a)$ .

recent work on the same system sees no evidence for saturation.<sup>24</sup> Since the isomerization motion involves only motion of a part of the molecule, the saturation region may occur at lower viscosity and this may explain the weaker dependence of the isomerization rate on viscosity in the higher viscosity (larger) alcohols. If such a boundary condition effect is operating in our data, it cannot simply be the result of relative solute-solvent size since we vary the viscosity by changing the temperature as well as the solvent and see good reproducibility of the reduced rate at a certain viscosity regardless of the manner in which the viscosity is produced.

A saturation effect is also predicted in the rotational friction coefficient of a rough hard sphere with partial slip boundary condition as a result of microscopic boundary layer effects.<sup>25</sup> The rotational friction coefficient takes the form

$$\zeta_{\text{rot}} = \frac{8\pi\eta_s R^3}{1 + 3\eta_s/\beta}, \quad (16)$$

where  $R$  is the hydrodynamic radius and  $\beta$  is the slip coefficient. In fact, using an expression for the friction of the form of Eq. (16) in Eq. (3) will reproduce the shallow dependence of rate on viscosity at higher viscosities. However, in view of the lack of any clear experimental demonstration of such an effect even at very much higher viscosities than those studied here, we do not consider that the deviations we observe are due to a boundary condition effect. Rather, for reasons discussed below, we conclude that the deviations are intimately related to the existence of a barrier to isomerization, or at least to the nature of the intramolecular potential surface.

#### E. Internal potential surface and viscosity dependence

In Table IV, we present data on isomerization rates for three molecules. Data are presented for change of electronic state (DODCI) and solvent type (DPB). All the data were obtained in our laboratory except for those on fast acid violet (FAV) which were obtained from Ref. 16. The barrier height and effective fre-



quency ( $k_{iso}^*$ ) vary over a considerable range for the different systems. Examples of both intermediate friction ( $\omega' \tau_v \sim 1$ ) and the Smoluchowski limit ( $a \sim 1$ ) occur.

There are several important observations to be made about the data presented in Table IV. First, within a single molecular species, a smaller barrier implies a smaller reduced rate or effective frequency  $k_{iso}^*$ . In the case of DODCI, overall rotational motion is taken to be a "barrierless" case of microscopic motion to be compared to isomerization. In DPB the internal barrier as deduced from isoviscosity plots, is drastically reduced in polar solvents. FAV is reported to have a very small barrier.<sup>16</sup>

Second, a larger barrier implies a less strong dependence on viscosity, as measured by  $a$  or the product  $\tau_v \omega'$ . In barrierless cases, the Smoluchowski limit of a  $1/\eta$  dependence is approached. [This is true even for the FAV case which has been claimed to obey the Forster relation  $k \propto \eta^{2/3}$ .<sup>16</sup> Our own plots of published data for this molecule<sup>16</sup> fit well to  $(1/\eta)^a$  with  $a = 0.97$ .]

It seems likely that as the barrier gets smaller, the curvature at the top will get flatter and hence the frequency  $\omega'$  will get smaller, for any reasonable model of the potential surfaces. Thus, the observation that an increasing barrier implies shallower viscosity dependence is consistent with the notion that high barrier cases are more potential controlled or inertial, and low barrier cases are more diffusive or viscosity controlled.

If it is true that the viscosity dependence of a given process can be changed to fit a simple hydrodynamic form ( $1/\eta$ ) by a modification of the internal barrier it seems unlikely that the form of the viscosity dependence is determined by the details of solvent-solute coupling: a change in the internal potential surface cannot change hydrodynamic boundary conditions. Unfortunately, the data in Table IV are not as definitive as we would like since in each case other factors such as solvent or molecular type or electronic state change. However, we consider that the data in Table IV provide a strong indication that the intramolecular potential surface is a major influence in the viscosity dependence of the isomerization process.

The observation that the reduced rate decreases with decreasing barrier is also consistent with the idea that the isomerization becomes more viscosity controlled for the low barrier cases, i.e., the reaction coordinate spends more time in the barrier crossing region and is thus more likely to have its velocity reversed before coming under control of the forces which pull it to the product configuration.

We should mention at this point that in the one-dimensional barrier crossing theory, if the barrier height ( $E_0$ ) is less than  $kT$ , the notion of a time independent rate constant breaks down.<sup>18</sup> If this effect is present in DPB in alcohol solvents or FAV, the interpretation of the observed decay time may be ambiguous. However, single exponential decay is observed in both

cases and we thus assume that rate theory is still applicable to these systems.

## F. Frequency dependent friction

One way to explain both the influence of potential surface on the viscosity dependence and the actual breakdown of Eq. (7) is to invoke a breakdown of a more fundamental assumption of Fokker-Planck theories: the assumption of Markovian friction.

The only authors who have discussed frequency dependent friction in the context of the barrier crossing problem are Grote and Hynes<sup>19</sup> who have suggested that when the forces on the isomerization coordinate relax on a time scale comparable to the velocity relaxation time, the frequency dependent friction  $\zeta(\omega)$  should be evaluated at the reactive frequency  $\lambda_r = 2\pi k_{iso}^*$ . In the simple case when the well curvature and the barrier curvature are equal, Grote and Hynes found that  $k_{iso}^*$  and  $\zeta(\omega)$  obey the self-consistency relation

$$k_{iso}^* = \frac{1}{2\pi} \frac{\omega'^2}{2\pi k_{iso}^* + \zeta(2\pi k_{iso}^*)/\mu} \quad (17a)$$

This result can easily be generalized to the case of unequal  $\omega_0$  and  $\omega'$ :

$$k_{iso}^* = \frac{1}{2\pi} \frac{\omega_0^2}{2\pi k_{iso}^* + (\omega_0/\omega') [\zeta(2\pi k_{iso}^*)/\mu]} \quad (17b)$$

In the molecules studied here  $k_{iso}^* \sim 10^{11} - 10^{12} \text{ s}^{-1}$  and so  $\zeta(2\pi k_{iso}^*)$  may differ significantly from its zero frequency value. If the force correlation time is comparable to  $k_{iso}^*$  the effective friction will, in general, be different than if the isomerization coordinate felt a representative sample of forces in a time period  $k_{iso}^{*-1}$ . It should be noted that this expression cannot be valid in the low friction limit since it implies that the rate approaches the transition state value  $2\pi k_{iso}^* \sim \omega_0$ .

Equation (17) cannot be applied to our experimental data in a simple way to yield the form of  $\zeta(2\pi k_{iso}^*)$ . The reason for this difficulty arises from the experimental necessity of changing viscosity in order to change  $k_{iso}^*$ . Thus, although simple inversion of Eq. (17) yields (for  $\omega' = \omega_0$ )

$$\frac{\zeta(2\pi k_{iso}^*)}{\mu} = \frac{\omega'^2}{2\pi k_{iso}^*} - 2\pi k_{iso}^* \quad (18)$$

Application of Eq. (18) to our data will not give the form of  $\zeta(2\pi k_{iso}^*)$  because each value of  $k_{iso}^*$  we measure corresponds to a different  $\eta$  [or  $\zeta(0)$ ]. Rather, application of Eq. (18) gives the form of  $\zeta(\eta, 2\pi k_{iso}^*)$  which is necessary to make our data fit (17). The difficulty cannot be resolved by simply normalizing each point by dividing it with the viscosity since the theory of Bixon and Zwanzig<sup>27</sup> for frequency dependent viscosity shows that it is incorrect to factor  $\zeta(2\pi k_{iso}^*)$  into the product of the viscosity and a frequency dependent factor. If a simple, few parameter model for  $\zeta(2\pi k_{iso}^*)$  were available, an iterative fit of Eq. (17) could be made. We have not attempted such a procedure. Instead, we have

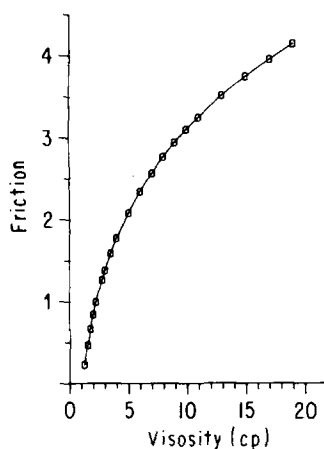


FIG. 7. Plot of friction vs viscosity for the DODCI excited state isomerization. The curve was obtained using Eq. (18).

used Eq. (18) with our data to construct a plot of friction vs viscosity. Figure 7 shows such a plot for the DODCI ground state data. This curve was obtained using the parameters of the best fit of  $B/\eta^a$  to our data and a value of  $\omega'$  ( $=\omega_0$ )  $= 2.45 \times 10^{13} \text{ s}^{-1}$  as obtained from the best fit to Kramers equation. At high viscosities there is a roughly linear dependence of friction on viscosity but as viscosity decreases the friction falls much more rapidly than linearly.

A strong qualitative feature of Eq. (17) is that, as the high friction limit is approached,  $k_{\text{iso}}^* \sim 1/\xi(0)$  which implies that  $k_{\text{iso}}^* \sim 1/\eta$  if  $\xi(0) \propto \eta$ . This means that our data cannot continue to decrease more slowly than  $1/\eta$  as we increase  $\eta$  to larger and larger values. At some range of viscosity there must be a transition to  $1/\eta$  if the Grote and Hynes theory is valid. On the other hand, it is possible that the connection between barrier crossing rate and the zero frequency friction is a peculiar feature of Kramers-type theories rather than a necessary one. Experiments at much higher viscosities will be necessary to establish if and when a transition to a  $1/\eta$  dependence takes place.

Recently, Oxtoby and Bagchi<sup>28</sup> have calculated the isomerization rate via the Grote and Hynes expression using the Bixon-Zwanzig form<sup>27</sup> for the frequency dependent friction. A general feature of the calculations using pure slip or pure stick boundary conditions is that the viscosity dependence is well described by  $k_{\text{iso}}^*/\eta^a$  with  $0.1 < a < 1.0$  (cf. the dashed line in Fig. 5). Thus, a frequency dependent friction may provide a rationale for the commonly observed fractional viscosity dependence of large amplitude motion radiationless transitions. The calculations show that a barrier frequency similar to our experimental values (e.g., the Kramers fit for DODCI excited states gives  $\omega_0 = 6.0 \times 10^{12} \text{ s}^{-1}$ ) produces significant deviations from Kramers theory. Also consistent with our experimental findings (Table IV) is the result that as  $\omega'$  increases, the value of  $a$  decreases. Calculations were also carried out using a partial slip boundary condition. As expected from the form of Eq. (16), this type of boundary con-

dition can also produce the sharp curvature and functional dependence on viscosity observed in the experiments without inclusion of a frequency dependent friction. However, for the reasons discussed above, we consider that a frequency dependent friction related to the sharpness of the intramolecular potential barrier provides the most consistent explanation of our results.

## V. CONCLUDING REMARKS

We have shown that in DODCI, the reduced rate of isomerization in both ground and excited states is well correlated with solvent viscosity in the series of linear alcohols. This result is much like that obtained for DPB in linear alkanes. Both molecules show an isomerization rate whose viscosity dependence is not well described by a hydrodynamic approximation to Kramers expression. Using the rotational friction as a direct measure of the isomerization friction for DODCI does not improve the fit. The dependence of  $k_{\text{iso}}^*$  on viscosity could be explained by the one-dimensional Kramers model, when the frequency dependence of the medium response is taken into account. The kind of behavior observed appears general for reduced rates of about  $10^{12} \text{ s}^{-1}$  in our solvents and temperatures. Two systems with reduced rates of  $< 10^{11} \text{ s}^{-1}$  show simple Smoluchowski viscosity dependence. We suggest that the shape of the intramolecular potential surface is responsible for the two types of behavior. Molecules with large (sharp) barriers probe a higher frequency region of the solvent viscosity than those with low (flat) barriers. To verify this conclusion, experiments are needed which span the intermediate and high friction regions since, at low enough isomerization rates, one ought to obtain the zero frequency friction limit, provided a hydrodynamic description is adequate. For studies performed over a wide enough range, we would expect to see a transition from the intermediate to high friction limit if the theory of Grote and Hynes<sup>19</sup> is valid. As mentioned earlier in the text, the frequency dependent friction is only one aspect of the theory which may fail. The success of the frequency dependent friction could be fortuitous and the slow dependence of  $k_{\text{iso}}^*$  on the viscosity at high viscosities could be caused by other modes of relaxation becoming dominant, i.e., by the inadequacy of the one-dimensional Kramers theory. We feel that our data favors the frequency dependent friction explanation, but further work is clearly necessary before the reasons for the breakdown of Kramers equation can be definitely stated.

As a final point, we note that the process which has the slowest observed rate; DODCI ground state isomerization ( $\sim 3 \text{ ms}$ , ethanol,  $25^\circ \text{C}$ ) requires a frequency dependent friction to explain the observed behavior, whereas the fastest rate we have studied, DPB excited state isomerization ( $\sim 60 \text{ ps}$ , ethanol,  $25^\circ \text{C}$ ), only requires that we use the zero frequency limit of the friction. This behavior results because of the effects of the intramolecular potential. This result shows that high frequency motions and the frequency response of the medium could have important implications on chemical reactions which occur at modest rates.

## ACKNOWLEDGMENTS

This work was supported by NSF grant No. CHE 80-09216. Stephan P. Velsko was supported by a Harper Fellowship 1980-1981. We thank Dr. Biman Bagchi for many hours of informative discussion, Professor Robin Hochstrasser for showing us his stilbene data and for valuable discussions regarding the possible inadequacy of the one-dimensional model, and Dr. Thomas Gillbro and Dr. Villy Sundström for preprints of their work.

<sup>1</sup>S. P. Velsko and G. R. Fleming, *J. Chem. Phys.* **76**, 3553 (1982).

<sup>2</sup>H. A. Kramers, *Physica* **7**, 284 (1940).

<sup>3</sup>R. M. Hochstrasser (private communication).

<sup>4</sup>R. F. Grote and J. T. Hynes, *J. Chem. Phys.* **73**, 2715 (1980).

<sup>5</sup>B. Wilhelmi, *Chem. Phys.* **66**, 351 (1982).

<sup>6</sup>S. P. Velsko and G. R. Fleming, *Chem. Phys.* **65**, 59 (1982).

<sup>7</sup>D. H. Waldeck and G. R. Fleming, *J. Phys. Chem.* **85**, 2614 (1981).

<sup>8</sup>Landolt-Bornstein, *Zahlenwerte and Funktionen* (Springer, New York, 1967), Band II, Teil 5.

<sup>9</sup>D. N. Dempster, T. Morrow, R. Rankin, and G. F. Thompson, *J. Chem. Soc. Faraday Trans. 2* **68**, 1479 (1972).

<sup>10</sup>F. S. Swed and C. Eisenhart, *Ann. Math. Stat.* **14**, 66 (1943).

<sup>11</sup>J. Jaraudias, *J. Photochem.* **13**, 35 (1980).

<sup>12</sup>C. Rulliere, *Chem. Phys. Lett.* **43**, 303 (1976).

<sup>13</sup>K. M. Keery and G. R. Fleming, *Chem. Phys. Lett.* (in press).

<sup>14</sup>T. H. Forster and G. Hoffman, *Z. Phys. Chem. N. F.* **75**, 63 (1971).

<sup>15</sup>G. Gegiou, K. A. Muzkat, and E. Fisher, *J. Am. Chem. Soc.* **90**, 12 (1968).

<sup>16</sup>(a) C. J. Tredwell and A. D. Osborne, *J. Chem. Soc. Faraday Trans. 2* **76**, 1627 (1980); (b) A. D. Osborne, *J. Chem. Soc. Faraday Trans. 2* **76**, 1638 (1980).

<sup>17</sup>J. L. Skinner and P. G. Wolynes, *J. Chem. Phys.* **69**, 2143 (1978).

<sup>18</sup>J. Montgomery, D. Chandler, and B. Berne, *J. Chem. Phys.* **70**, 4056 (1979).

<sup>19</sup>R. F. Grote and J. T. Hynes, *J. Chem. Phys.* **74**, 4465 (1981).

<sup>20</sup>S. Chandrasekhar, *Rev. Mod. Phys.* **15**, 1 (1943).

<sup>21</sup>T. Gillbro and V. Sundström, *J. Phys. Chem.* **86**, 1788 (1982).

<sup>22</sup>P. S. Hubbard, *Phys. Rev.* **131**, 1155 (1963).

<sup>23</sup>S. A. Rice and G. Kenney-Wallace, *Chem. Phys.* **47**, 161 (1980).

<sup>24</sup>R. S. Moog, M. D. Ediger, S. G. Boxer, and M. D. Fayer (preprint).

<sup>25</sup>J. T. Hynes, R. Karpal, and M. Weinberg, *J. Chem. Phys.* **70**, 1456 (1979).

<sup>26</sup>J. L. Dote, D. Kivelson, and N. Schwartz, *J. Phys. Chem.* **85**, 2169 (1981).

<sup>27</sup>R. Zwanzig and M. Bixon, *Phys. Rev. A* **2**, 2005 (1970).

<sup>28</sup>B. Bagchi and D. W. Oxtoby, *J. Chem. Phys.* (submitted).